

Statistical Downscaling for the Projection of the Keetch Byram Drought Index in the Barito Basin

Nadia Farahnaz^{a1}, Arno Adi Kuntoro^{a2}, M. Syahril Badri Kusuma^b

^a Centre for Water Resources Development ITB, Jl. Ganesha 10 Bandung 40132, Indonesia
E-mail: ¹nadiafarahnaz@gmail.com; ²arnoak@ftsl.itb.ac.id

^b Faculty of Civil Engineering and Environment, Institute Teknologi Bandung, Jl. Ganesha 10 Bandung 40132, Indonesia
E-mail: msbadrik@yahoo.com

Abstract— Over the last few decades, prolonged drought in Indonesia has led to a catastrophic wildfire hazard, including on Kalimantan Island. The Barito River basin is one of the major river basins on the island, located in South and Central Kalimantan Provinces. According to The Indonesian National Board for Disaster Management (BNPB), the drought hazard index in the southern part of Kalimantan is mostly at the medium to high-risk level. In terms of Integrated Water Resources (IWRM), more detailed drought risk analysis needs to be conducted at the river basin level, so that drought adaptation and mitigation strategies can be integrated into long-term river basin management plans. In this study, a drought projection of the Barito River basin was simulated by using the Coupled Model Intercomparison Project 5 (CMIP5). A coarse grid of CMIP5 data was statistically downscaled to a smaller grid over the basin area. Data from climatology observation stations and Climate Forecast System Reanalysis (CFSR) were used to calibrate the bias correction function of the CMIP5 data. This function for rainfall data was developed based on the rainfall probability curve, while the bias correction function for temperature data was developed based on the elevation-temperature relation. The bias-corrected rainfall and temperature data were used as input for the Keetch-Byram Drought Index (KBDI) analysis. The study shows that the potential for drought hazard may increase in the future. Drought projection in the Barito basin for 2050 using KBDI shows that the potential areas with medium and high drought risk may cover around 50% and 2%, respectively, or about 35,000km² and 1,400km². The occurrence of wildfires also has a strong correlation with the drought index. A comparison between 1998 and 2015 fire hotspot data shows that most hotspots were located in areas in the medium and high drought risk categories. The study shows the importance of climate change impact analysis to prevent more catastrophic hazards in the future, especially in the Barito River basin, Kalimantan Island.

Keywords— Barito basin; climate change; statistical downscaling; keetch-byram; drought index.

I. INTRODUCTION

Over the last few decades, climate change has led to more catastrophic droughts and forest fires. Although anthropogenic factors contribute greatly to fire hazard, a combination of forest clearance by fire and natural factors such as low soil moisture and low rainfall might lead to a higher rate of forest fires [1]–[3]. Kalimantan is the island with largest tropical forest cover in Indonesia. However, rapid forest degradation since the 1970s has reduced this coverage from 71% in the 1980s to 54% in the 2000s [4]. Such degradation also leads to an increase in the forest fire hazard [5], [6]. One example is the long drought in Indonesia, which occurred during the El Niño event of 1997-1998, and was followed by fires which destroyed 8 million hectares of forest [7]. Two provinces that experience drought frequently are South Kalimantan and Central Kalimantan. Based on

information from the Banjarbaru Meteorological Agency in South Kalimantan, the drought risk in this area is relatively high. From early 2015 to 31st August 2015, no rain fell for 60 to 76 days in almost all areas of this part of the island. Because drought has extensive and multi-sectoral negative effects (economy, health, education, food, etc.), citizens and government need to have information about drought projections so that mitigation and adaptation plans can be implemented in advance [8].

Many methods have been developed to estimate climate parameters for hydrological simulations; for example, the stochastic approach [9], trendlines and satellites [10], [11], and GCM [12], [13]. Several studies have used the output of climate change simulation scenarios for drought analysis, such as Li et al [14]. The purpose of this study is to simulate the projection of climate change effects on drought risk in the Barito basin up to 2050. This will assist the government

in mitigation and adaptation plans to minimize the losses caused by climate change, especially drought, in Indonesia.

II. MATERIALS AND METHOD

The study consists of three main parts: 1) bias correction of rainfall data obtained from the Climate Forecast System Reanalysis (CFSR) and the National Centres for Environmental Prediction (NCEP); 2) statistical downscaling of global climate model output for the case study of the Barito basin; and 3) drought index analysis using the Keetch-Byram Drought Index (KBDI).

A. KBDI

KBDI is a drought index developed for the purpose of forest fire control in Florida, USA [15]. The index represents the drought level of soil moisture, which is calculated based on daily weather data. The index ranges from 0 to 800 if rainfall is measured in inches, and 0 to 2000 if measured in mm. The value of KBDI is calculated based on the following equation:

$$\text{today KBDI } (Q^t) = \sum \text{yesterday KBDI} - (10R) + DF \text{ today} \quad (1)$$

where:

R = net rainfall

DF = modified drought factor used to estimate fire hazard, with the following formulation:

$$DF = \frac{(2000 - YKBDI)(0.9676^{(0.0875 \times T_{max} + 1.552)} - 8.229)}{(1000)(1 + 10.88^{(-0.00175 \times \text{Annual})})} \quad (2)$$

where:

YKBDI = yesterday's drought index

T_{max} = maximum temperature ($^{\circ}\text{C}$)

Annual = average annual rainfall (mm)

KBDI is widely used in drought and forest fire studies. For example, it was employed to estimate the spatial and temporal variability of forest fire potential in Lebanon [16]. In other case studies, KBDI and EVI were used to assess the effect of the seasonal variability of precipitation and drought on paddy fields in Indonesia [17], while KBDI (with adjustment for local climate) and the water table effect were used to assess forest fire hazard in tropical wetlands [18].

B. Data collection

CFSR provides gridded data of climate parameters, such as daily temperature and rainfall, and has been used in many studies; for example, Darfia et al [19]. This study uses daily rainfall data, daily temperature, daily average temperature, daily maximum temperature, and the elevation of the climatological station. The satellite rainfall data were taken from CFSR data, with 74 grids within the Barito basin area. The GCM output used was the multi model means of the Coupled Model Intercomparison Project Phase 5 (CMIP5) compiled by the Netherlands Meteorological Agency (KNMI), for RCP scenario 6. There are six grids (grid size = $2.5^{\circ} \times 2.5^{\circ}$) of the GCM data located in the Barito basin, as shown in Figure 1.

C. Bias Correction of CFSR Rainfall Data

Bias correction is used to match the statistical characteristics of coarse grid satellite or GCM output with

the data from climatological stations (observational data). There are several examples of studies related to the application of the bias correction method; for example, using bias correction based on quantile mapping to adjust GCM and RCM output in South East Asia [20], and its use to correct TRMM data for drought index analysis in Central Java, Indonesia [21].

In this study, bias correction was used to adjust CFSR for further use in the Barito basin. Since the northern part of the basin has a limited number of meteorological stations, the corrected CFSR data were used to ensure that the drought index for areas with limited or no fixed data could be calculated. A comparison between observational and CFSR data was conducted within one GCM grid. The rainfall probability curve for both sets of data was compared to determine the correction function of the CFSR data. This process was conducted to ensure that the corrected CFSR data had similar statistical characteristics to the available observed data by applying the correction function on the rainfall probability density curve.

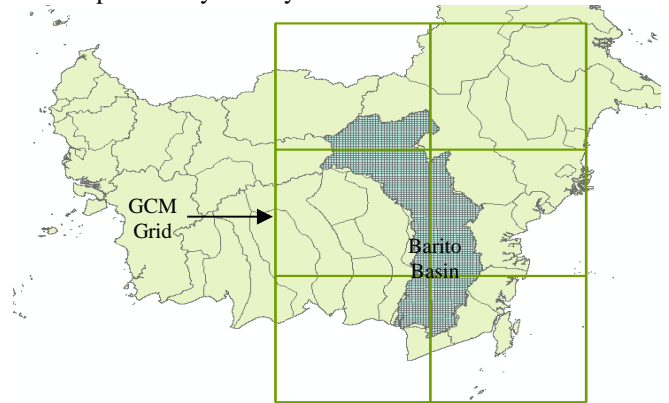


Fig. 1 GCM grid in Barito basin

D. Statistical Downscaling of GCM Rainfall and Temperature Output

Rainfall and temperature data from a GCM grid size of $2.5^{\circ} \times 2.5^{\circ}$ (about 300km^2) were statistically downscaled to CFSR grid size (about 33.3km^2). The timescale of the downscaled data is monthly, while calculation of the drought index using KBDI employed daily data. Therefore, stochastic analysis was conducted to generate daily rainfall series based on monthly rainfall from the probability curve of historical daily rainfall data.

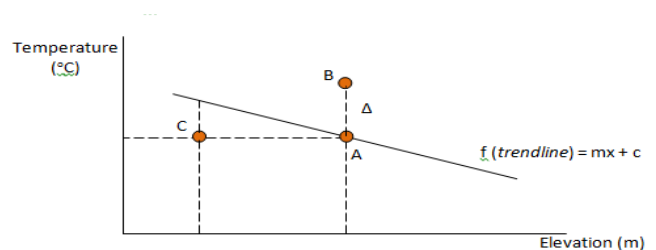


Fig. 2 Relation between temperature and elevation

Temperature downscaling was conducted based on the relationship between the elevation of the station and the average observational temperature on each grid at the station, so that the equation of the trend-line curve could be obtained. Figure 2 shows the relationship between temperature and

elevation, where delta (Δ) represents the difference between the average temperatures in RCP in grid (B) and the temperature of the average grid elevation (A). C is the GCM temperature, which is calculated in the n^{th} year.

Equation (3) is used as a correction function of the GCM temperature output:

$$T = [f(\text{trendline}) + \Delta - A + C] \quad (3)$$

where:

T = corrected temperature in n^{th} year

Δ = difference between A and B

A = temperature at average grid elevation

B = average temperature in RCP on grid

C = GCM temperature data in n^{th} year

The corrected average monthly temperature data were then linearly interpolated into daily data based on the assumption that average monthly temperatures occur in the middle of the month (15th day).

E. Comparison between KBDI and fire hotspot data

The spatial distribution of the computed KBDI was compared with the fire hotspot data in Barito basin from the same year. In this case, hotspot data from 1998 and 2015 were used.

III. RESULTS AND DISCUSSION

F. Bias Correction of CFSR Rainfall Data

The correction factor was obtained by comparing the CFSR rainfall probability curve and the observational data within the same period. Due to limited observational data, the above comparison was conducted using different periods. Grids one and two use data from 1999 to 2005; grid three uses data from 2000 to 2012, while grid four use data from 1994 to 2004. The results of the above comparison were four sets of equations, which were applied to each grid. An example of a set of equations for grid 1 is shown in Figure 3

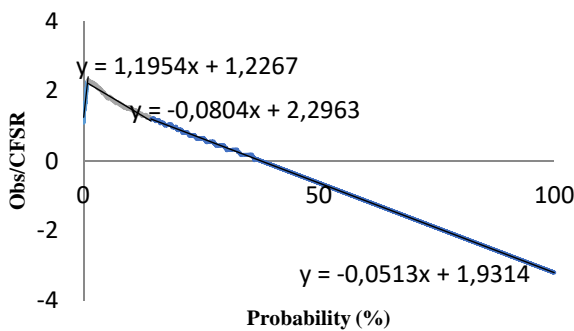


Fig. 3 Rainfall probability in grid 1

From the trend-line equation on the probability of rainfall occurrence, the values of coefficients m and c for linear function $y = mx + c$ can be obtained, which are shown in Table I. A comparison between CFSR and observational data (before and after correction) can be seen in Figure 4. Figure 4A shows a wide gap between the CFSR rainfall probability curve and the observational data, while Figure 4B shows the coincidence of the curve and data. The coinciding curves show that the corrected CFSR data and observational data have similar statistical characteristics, meaning that the corrected CFSR can be used to represent

historical rainfall data in the Barito basin for the drought analysis.

TABLE I
RAINFALL CORRECTION FACTORS

GRID 1					
Prob < 1%		1% < Prob > 14.35%		Prob > 14.35%	
m	c	m	c	m	c
1.1954	1.2267	-0.0804	2.2963	-0.0513	1.9314
GRID 2					
Prob < 0.95%		0.95% < Prob > 9.87%		Prob > 9.87%	
m	c	m	c	m	c
0.5641	1.273	-0.092	1.8422	-0.0247	1.1644
GRID 3					
Prob < 4.35 %			Prob > 4.35 %		
m	c	m	c	m	c
0.2022	0.9924	-0.073		2.328	
GRID 4					
Prob < 2.43%		2.43% < Prob > 20%		Prob > 20%	
m	c	m	c	m	c
0.2901	1.0638	-0.0569	1.7217	-0.0493	1.669

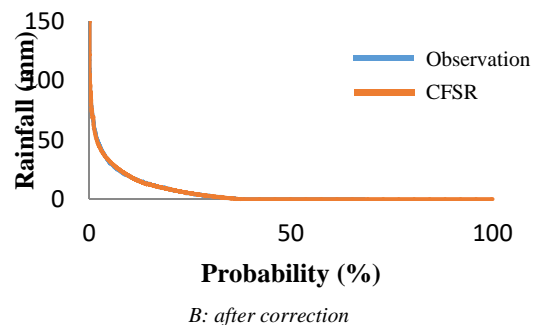
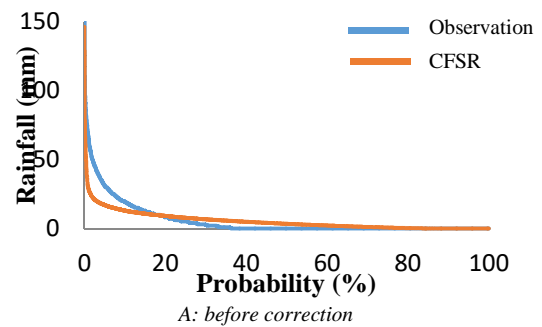


Fig. 4 Rainfall probability curve in grid 1 before and after correction

The corrected value for each grid is assumed to be valid in the middle of the grid. Therefore, it is necessary to interpolate the correction factor by using the spatial averaging method. In this study, the Inverse Distance Weight (IDW) method was used, which takes the distance of each CFSR grid to the midpoint of the GCM grid. An example plot of the corrected CFSR rainfall in the Barito basin is shown in Figure 5.

G. Statistical Downscaling of GCM Data

Monthly GCM output from the multi-model mean of CMIP5 was used as input for analysis of future rainfall and temperature trends. The comparison between GCM output and historical data also shows a wide gap. Therefore, the same bias correction method procedure was also applied to

the GCM output by comparing monthly GCM data and the corrected CFSR from 1979 to 2013.

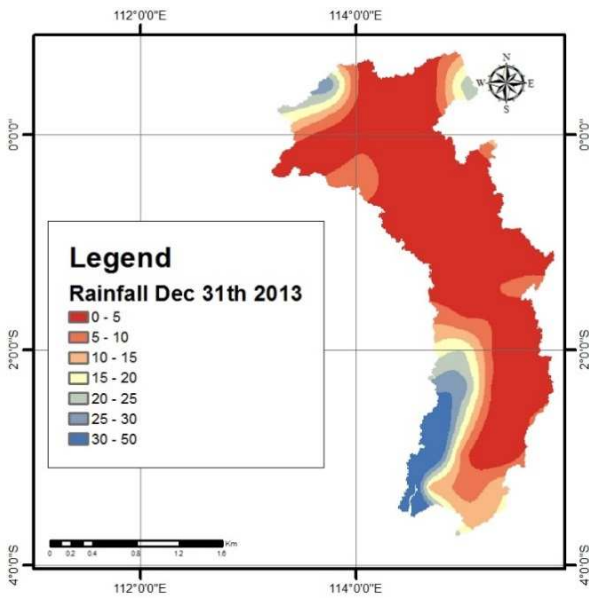


Fig. 5 CFSR Rainfall distribution December 31, 2013

Since KBDI use daily time series, stochastic analysis was made to generate daily series from monthly data of the GCM output. Daily rainfall series were generated based on the trend of the number of rainy days in a month at the available rainfall observation station. The approach used to generate daily rainfall from the corrected GCM output is as follows:

$$prob_{month} = \frac{n_{rain}}{n_{day}}$$

$$x = rand(0 - 1)$$

$$rain_{day} = \begin{cases} \gamma^{-1}(\alpha, \beta, x); & \text{for } x < prob_{month} \\ 0; & \text{for } x \geq prob_{month} \end{cases}$$

$$rain_{month}' = \sum_{d=1}^{n_{day}} rain_{day}$$

$$rain_{day}' = rain_{day} \frac{rain_{month}}{rain_{month}'}$$

where:

$prob_{month}$ = the probability of rainfall occurrence in a month

x = a random figure between 0 and 1

n_{rain} = the average number of rain days in a month

n_{day} = the number of days in a month

$\gamma^{-1}(\alpha, \beta, x)$ = the Inverse Gamma Distribution of daily rainfall in upper CRB.

The plot of monthly rainfall and number of rainy days from the available station data, which were used as the basis for the stochastic analysis, is shown in Figure 6. By assuming that monthly rainfall is linear with the number of rainy days in a month, the trend-line equation in Figure 6 can be used to estimate the number of rainy days from the monthly rainfall data. For example, in the wet season, with rainfall of 600mm/month, the estimated number of rainy days is 23, while in the dry season, with rainfall 100mm/month, the estimated number of rainy days is 8.

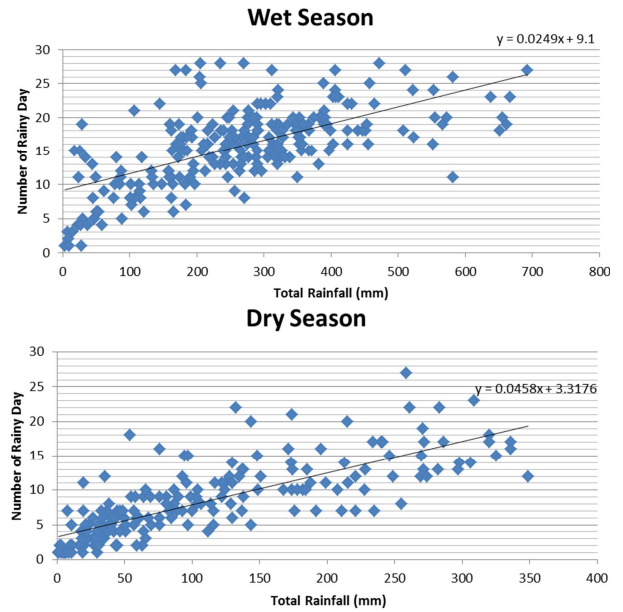


Fig. 6 Monthly rainfall vs rainy days in wet and dry seasons in the Barito basin

Output examples of the downscaled rainfall and temperature are shown in Figures 7 and 8. Figures 7 and 8 show that the upstream part of the Barito basin tends to have higher monthly rainfall (300-600mm/month) and lower average temperature (15-22.5°C). Meanwhile, the downstream part of the basin tends to have lower monthly rainfall (0-200/month) and higher average temperature (22.5-30°C). From the above trends, it is expected that the downstream part has a higher risk of drought than the upstream.

H. KBDI analysis

KBDI values were calculated on daily basis to obtain the average monthly values. The data used to calculate these values started from January 1st each year, up to the last year of rainfall and temperature statistical downscaling data. Examples of the KBDI analysis results from CFSR grid 50 are shown in Tables II and III.

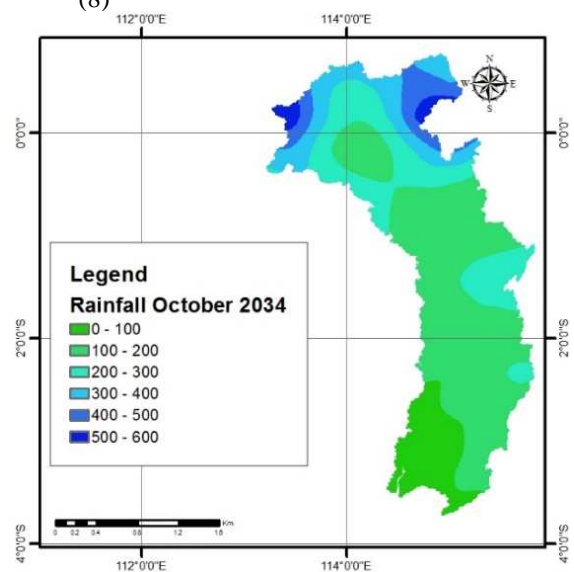


Fig. 7 Output example of downscaled GCM rainfall in the Barito basin

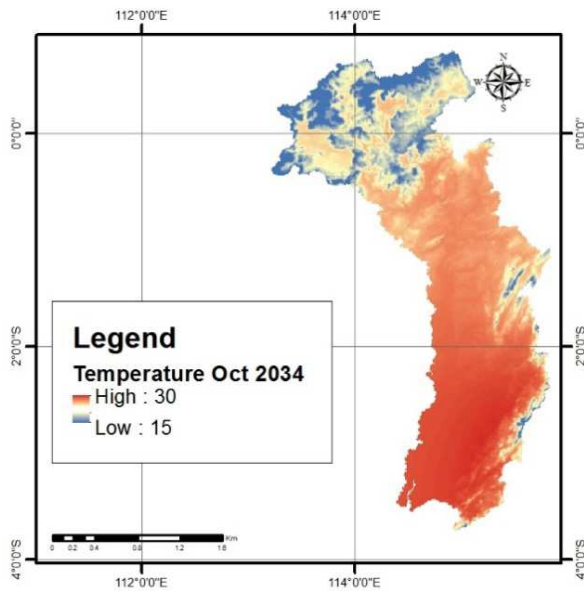


Fig. 8 Output example of downscaled GCM temperature in the Barito basin

TABLE II

OUTPUT EXAMPLE OF MONTHLY KBDI VALUES IN THE BARITO BASIN

Year	Jan	Feb	Mar	Apr	May	Jun	Jul	Aug	Sep	Oct	Nov	Dec
1997	-	387	793	1138	1096	1101	1292	1433	1549	1549	1586	1507
1998	1290	882	1140	1226	1139	1229	1043	1345	1572	1492	1599	1251
2031	76	665	956	1059	1182	1184	1266	1380	1622	1663	1633	1349
2032	1294	1115	1058	1362	1009	1170	1288	1629	1527	1625	1622	1511
2033	1521	1090	1207	1168	1272	1226	1209	1394	1599	1699	1647	1364
2034	1308	1041	1035	1336	853	983	1113	1487	1584	1729	1750	1479
2035	1228	1179	1061	1128	974	1272	1288	1574	1597	1595	1633	1436
2046	-	434	914	907	1146	1228	1297	1396	1643	1787	1769	1576
2047	1119	1078	1233	1244	1028	1193	1278	1447	1574	1703	1489	1424
2048	1219	1009	1149	1135	1156	1336	1337	1354	1573	1760	1770	1448
2049	1147	1033	1048	1169	1103	1088	1378	1402	1519	1689	1707	1454
2050	1233	1286	1049	1382	983	1219	1190	1620	1395	1667	1647	1399

TABLE III

OUTPUT EXAMPLE OF DROUGHT CLASSIFICATION IN THE BARITO BASIN

Year	Jan	Feb	Mar	Apr	May	Jun	Jul	Aug	Sep	Oct	Nov	Dec
1997	L	L	M	M	M	M	M	M	H	H	H	M
1998	M	L	M	M	M	M	M	M	H	M	H	M
2031	L	L	L	M	M	M	M	M	H	H	H	M
2032	M	M	M	M	M	M	M	M	H	H	H	H
2033	H	M	M	M	M	M	M	M	H	H	H	M
2034	M	M	M	M	L	L	M	M	H	H	X	M
2035	M	M	M	M	L	M	M	M	H	H	H	M
2046		L	L	L	M	M	M	M	H	X	X	H
2047	M	M	M	M	M	M	M	M	H	H	M	M
2048	M	M	M	M	M	M	M	M	H	X	X	M
2049	M	M	M	M	M	M	M	M	H	H	H	M
2050	M	M	M	M	L	M	M	M	H	M	H	M

Notes: L=low, M=medium, H=high, X=extreme

I. Comparison between KBDI and hotspot data

The drought indices of 1998 and 2015, calculated by using the corrected GCM data, were compared with hotspot data from the same year. A comparison between KBDI and the hotspot data is shown in Figure 9.

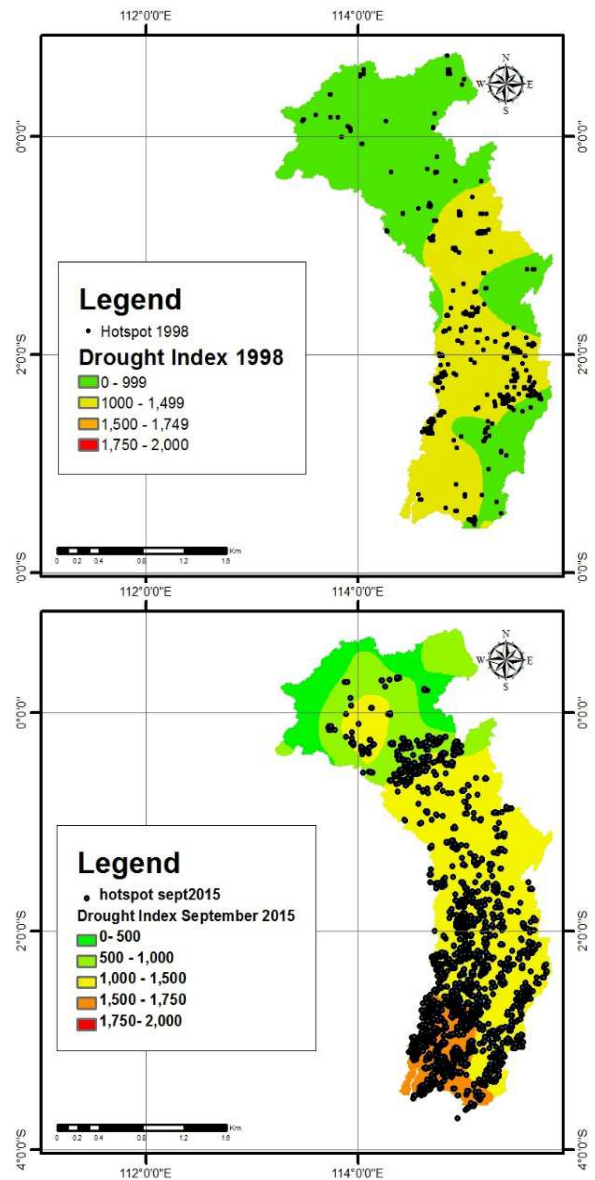


Fig. 9 Comparison between KBDI and fire hotspots in 1998 and 2015

Figure 9 shows that although hotspots also occur in areas with a low category drought index, most occur in areas in the medium and high categories. For example, in 2015, most hotspots occurred in the southern part of the Barito basin in areas corresponding to the medium to high drought index. The above comparison shows that even in the medium category, the occurrence of forest fires is relatively high. It also indicates that drought and fire hazards might increase more in the northern part of the basin.

J. Future drought projection

A drought projection was conducted by applying the corrected GCM rainfall and temperature data as input into KBDI computation from 2030 to 2050. Output examples of this projection are shown in Figure 10.

IV. CONCLUSION

GCM data can be used as input data for drought analysis after being corrected by observation station data. Direct use of GCM without applying such a correction factor may result in highly biased results. Drought analysis using KBDI shows relatively good correlation with historical drought data, as can be seen in comparison with the spatial and temporal distribution of hotspot data. The results of KBDI using the corrected GCM data from 1998 and 2015 as input correlate well with the hotspot distribution data. Therefore, the corrected GCM data can be used to project future droughts.

Droughts in the high and extreme categories tend to occur in the southern part of the Barito basin, while those in the medium category tend to be spread across the basin, from south to north. Only a small part of the mountainous area in the north of the basin shows a low drought index. The projected drought indexes up to 2050 indicate that medium drought risk might occur every year, with the greatest possibility in October and November. Hotspot data from 2015 show that even medium drought index hotspots may spread out over the basin. Therefore, it is necessary to develop appropriate integrated adaptation and mitigation strategies, together with improvements in monitoring systems, to prevent drought and forest fire disasters in the future.

REFERENCES

- [1] Keeley, JO, Syphard, AD. Climate Change and Future Fire Regimes: Examples from California. *Geosciences*. 2016; 6 (37).
- [2] Stevens-Rumann, CS., Kemp, K.B., Higuera, P.E., Harvey, B.J., Rother, B.T., Donato, D.C.et.al.: Evidence for declining forest resilience to wildfires under climate change. *Ecology Letters*, 21: 243–252, 2018.
- [3] Abatzoglou, JT, Williams, AP. Impact of anthropogenic climate change on wildfire across western US forests, *PNAS* Vol.113 No.42, (2016), 11770–11775.
- [4] Stibig, HJ, Malingreau, JP. Forest cover of insular Southeast Asia mapped from recent satellite images of coarse spatial resolution. *Ambio*, Vol.32 No.7, 469-475, 2003
- [5] Miettinen, J, Langner, A and Siegert, F. Burnt area estimation for the year 2005 in Borneo using multi-resolution satellite imagery. *International Journal of Wildland Fire*, Vol.16, 45-53, 2007
- [6] Langner, A., Miettinen, J., and Siegert, F.: Land cover change 2002–2005 in Borneo and the role of fire derived from MODIS imagery. *Global Change Biology*, Vol.13, 2329-2340, 2007.
- [7] Cochrane, MA. Fire science for the rainforest. *Nature*, Vol.421, 913-919, 2003.
- [8] Rossi, G., Vega, T., and Bonaccorso, D. (eds.), *Methods and Tools for Drought Analysis and Management*, 195–216, Springer, 2007
- [9] Lobo, GP., Frankenberger, J.R., Flanagan, D.C., Bonilla, C.A., Evaluation and improvement of the CLIGEN model for storm and rainfall erosivity generation in Central Chile, *Catena*, 127 (2015) 206–213.
- [10] Pombo, S, Oliveira, RP. Evaluation of extreme precipitation estimates from TRMM in Angola, *Journal of Hydrology* 523 (2015) 663–679.
- [11] Garcia-Pintado, C., Mason, D.C., Dance, S.L, Cloke, H.L., Neal, J.C., Freer, J., and Bates, P.D., Satellite-supported flood forecasting in river networks: A real case study, *Journal of Hydrology* 523 (2015) 706–724.
- [12] Islam, Z, Gan, TW. Potential combined hydrologic impacts of climate change and El Niño Southern Oscillation to South Saskatchewan River Basin, *Journal of Hydrology* 523 (2015) 34–48.
- [13] Cavalcanti, I.F.A., Carril, A.F., Penalba, O.C., Grimm, A.M., Menendez, C.G., et al., Precipitation extremes over La Plata Basin – Review and new results from observations and climate simulations, *Journal of Hydrology* 523 (2015) 211–230.

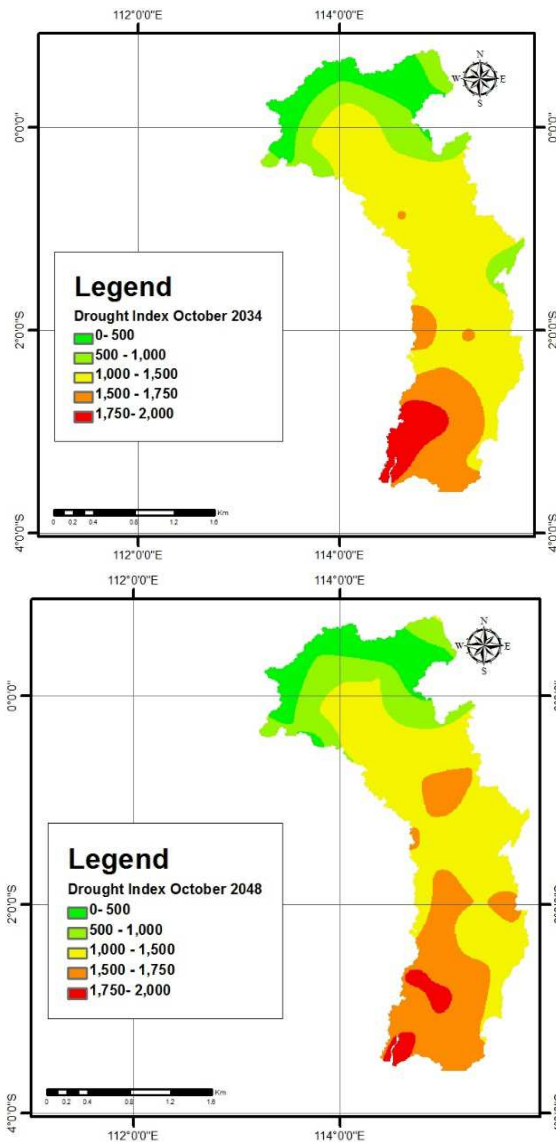


Fig. 10 Output example of drought projection in 2034 and 2048

Drought projection for the 2030s (October 2034 is taken as an output sample) shows the areas in the high category drought index in the southern part of the Barito basin. Meanwhile, the projection for the period of the 2040s (October 2048 is taken as sample output) shows an increase in areas within the high category drought index in the central part of the basin.

The projection of the drought index from 2046 to 2050 shows that high levels will increase by 1,400 km² compared to the period 2031-2035. The projection of the areas corresponding to the medium drought index tends to increase every year. By 2050, it is estimated that the medium drought index area will reach 35,000 km², which is more than 50% of the total basin area.

Drought evolves over a relatively long period. Appropriate adaptation and mitigation efforts, together with improvement in monitoring systems, might be effective in reducing its negative impacts in the future [8]. Water-saving technologies, water infrastructure development, increasing water productivity, and changes to crop systems might be a good adaptation strategy in the future [22].

- [14] Li, J., Zhang, Q., Chen, Y.D., Singh, V.P., Future joint probability behaviors of precipitation extremes across China: Spatiotemporal patterns and implications for flood and drought hazards, *Global and Planetary Change* 124 (2015) 107–122.
- [15] Keetch, J. J., and G. M. Byram. 1968. A Drought Index for Forest Fire Control. USDA. Forest Service Research Paper SE-38.
- [16] Mitria, G, Jazia, M, McWeth, D. Investigating temporal and spatial variability of wildfire potential with the use of object-based image analysis of downscaled global climate models, South-Eastern *European Journal of Earth Observation and Geomatics*, Issue Vo3, No2S, 2014.
- [17] Darmawan, S., Takeuchi, W., Shofiyanti, R., Sari, D.K., and Wikantika, K., Seasonal analysis of precipitation, drought and vegetation index in Indonesian paddy field based on remote sensing data, 7th IGRSM International Remote Sensing & GIS Conference and Exhibition, IOP Conf. Series: Earth and Environmental Science 20 (2014) 012049.
- [18] Taufik, M, Setiawan, BI, van Lanen, HAJ. Modification of a fire drought index for tropical wetland ecosystems by including water table depth, *Agricultural and Forest Meteorology* 203 (2015) 1–10.
- [19] Darfia, NE, Kusuma, MSB, Kuntoro, AA, Kajian Kelayakan Pemanfaatan Data CFSR dalam Analisis Indeks Kekeringan di DAS Rokan, Provinsi Riau (Study of CFSR Data Feasibility for Drought Index Analysis in Rokan Basin, Riau Province), Seminar Nasional Industri dan Teknologi (SNIT), Politeknik Negeri Bengkalis, 2016.
- [20] Ngai, ST, Tangang, F, Juneng, L. Bias correction of global and regional simulated daily precipitation and surface mean temperature over Southeast Asia using quantile mapping method, *Global and Planetary Change* 149 (2017) 79–90.
- [21] Levina, Kajian Koefisien Korelasi Indeks Kekeringan Berdasarkan Data Hujan Lapangan dan TRMM: Studi Kasus WS Pemali Comal, Jawa Tengah (Study of Drought Index Correlation Coefficient based on Observed Rainfall Data and TRMM: Case Study of Pemali-Comal Basin, Central Java), Thesis, Master Program in Water Resources Management, Institut Teknologi Bandung 2014.
- [22] Hijioka, Y, Lin, E, Pereira, JJ, Corlett, RT, Cui, X, Insarov, GE, et al. 2014: Asia. In: Climate Change 2014: Impacts, Adaptation, and Vulnerability. Part B: Regional Aspects. Contribution of Working Group II to the Fifth Assessment Report of the Intergovernmental Panel on Climate Change [Barros, V.R., C.B. Field, D.J. Dokken, M.D. Mastrandrea, K.J. Mach, T.E. Bilir, M., et al. (eds.)]. Cambridge University Press, Cambridge, United Kingdom and New York, NY, USA, pp. 1327-1370.